Active Suppression of Quantum Dephasing in Resonantly Driven Ensembles

C. He and R. R. Jones

Department of Physics, University of Virginia, Charlottesville, Virginia 22904-4714, USA

We have used quantum control to suppress the impact of random atom positions on coherent population transfer within atom pairs, enabling the observation of dipole-dipole driven Rabi oscillations in a Rydberg gas with hundreds of atoms. The method exploits the reduced coupling-strength sensitivity of the off-resonant Rabi frequency, and coherently amplifies the achievable population transfer in analogy to quasi-phase-matching in nonlinear optics. Simulations reproduce the experimental results and demonstrate the potential benefits of the technique to other many-body quantum control applications.

The ability to create and manipulate superposition states possessing well-defined relative amplitudes and phases is a key capability for controlling quantum systems. Typically, (near) resonant interactions play an essential role, enabling the transfer of probability amplitude between states to establish an initial coherence or entanglement, manipulate it, and/or measure it in a desired quantum operation. The application of a coherent coupling over a specific period of time creates a superposition in which the relative amplitude and phase of the constituent states is fully determined by the interaction strength and detuning from resonance. Thus, in an ensemble of nominally identical elements for which the interaction strength or detuning is nonuniform, the characteristics of the quantum state created (or modified) through the interaction will vary among the constituents. Alternatively, if the quantum state of interest involves multiple elements of the ensemble, such inhomogeneities can significantly impact the evolution of entanglement and the nature of the quantum state [1–6].

We have developed a control scheme that can substantially reduce the impact of inhomogeneities on quantum ensembles driven by (near) resonant interactions. The method is applicable when, for all elements, the relevant resonance occurs at the same value of some externally tunable parameter, but where the coupling strength varies. Common examples of this scenario include optical excitation of a spatially extended sample using a laser beam with a nonuniform spatial intensity distribution [7–9], or Förster-resonant interactions [10–12] between nonuniformly spaced Rydberg atoms in a frozen gas [13–19]. We focus on the latter.

Specifically, we have used coherent control of near-resonant dipole-dipole (DD) interactions in a cold, random many-atom Rydberg gas to actively suppress dephasing associated with the variation in the coupling strength between neighboring atoms. To implement the control, pulsed electric field sequences rapidly tune the eigenstates of Rb Rydberg atom pairs back and forth across a Förster resonance, holding the atoms in opposing wings of the resonance for equal times, substantially reducing the variation in the generalized Rabi frequency over the ensemble. The sequence results in a periodic reversal of the sign of the Rabi phase lag accrued in adjacent time intervals, amplifying the coherent population transfer in a time-domain analogy to spatial quasiphase matching schemes in nonlinear materials [20], and enabling what is to our knowledge the first observation of *DD-driven* Rabi oscillations in a random Rydberg gas with more than a few atoms [12]. The mechanism underlying the control can be understood using an analytic two atom model, but numerical simulations that include beyond nearest-neighbor interactions are required to obtain quantitative agreement with the experiments. Simulations also demonstrate the effectiveness of the technique for suppressing variations in the Rabi phase and, accordingly, in the quantum state distribution in spatially ordered Rydberg arrays with small residual differences in atom separation, such as those being employed for quantum simulation and computing applications [21–23].

In the experiments, a random ensemble of ~ 1000 $32p_{3/2}$, $|m_j| = 3/2$ ^{85}Rb Rydberg atoms is excited from a 70 μK magneto-optical trap using a 300 ns laser pulse [24]. Voltages applied to a pair of parallel plates straddling the magneto-optical trap facilitate the creation of an initial static, $F \simeq 12$ V/cm, and subsequent pulsed, electric fields within the excitation volume. Following the Rydberg excitation, electric field steps with fast (~ 2 ns) rise and fall times rapidly Stark tune the Rydberg atoms on, or about, the $32p_{3/2}$, $|m_j| = 3/2 + 32p_{3/2}$, $|m_j| = 3/2 \leftrightarrow 32s + 33s$ (i.e., $pp \leftrightarrow ss'$) Förster resonance near $F_0 = 11.5$ V/cm [16]. Time spent in the vicinity of the resonance enables coherent population transfer between pp and ss' atom pairs via an anisotropic DD interaction $V(R, \Theta) = r_{ps}r_{ps'}f(\Theta)/R^3$, where r_{ps} ($r_{ps'}$) are radial matrix elements between $32p$ and $32s$ ($33s$), R is the separation between the

atoms in each pair, and $f(\Theta)$ describes the anisotropy [40] in terms of the angle Θ between the internuclear and electric field axes [24]. After the atoms have interacted for the desired time, state-selective field ionization is used to measure the final population in different Rydberg states [41].

Figure 1 shows the pp to ss' population transfer probability (i.e., the ss' population normalized to the total Rydberg population) as a function of the tuning field, for a 500 ns interaction time and Rydberg density $\rho = 2 \times 10^9$ cm^{-3}. The agreement between the simulated ensemble and measured line shapes is reasonable. The simulation and experiment differ more in the line shape wings, where the transition probability is dominated by atom pairs with separations much less than average [19]. While the agreement there can be improved somewhat by modeling the effect of Rydberg blockade [42], which suppresses the excitation of the closest atom pairs, our principal measurements focus on interactions closer to resonance where blockade effects have negligible effect [24]. The half-width at half-maximum energy width of the ensemble cusp and 50% Lorentzian line shapes are identical, $E_0 = 2V_0$ ($\simeq 3$ MHz for $\rho = 1 \times 10^9$ cm^3), where V_0 is the angle averaged interaction strength at the most probable pair separation for a given density, $R_0 \simeq (2\pi\rho)^{-1/3}$.

The inset to Fig. 1 shows the predicted evolution of the ss' population when the atoms are tuned to the Förster resonance and allowed to interact for 500 ns. The curves corresponding to isolated atom pairs exhibit clear Rabi oscillations with frequencies $\gamma(R, \Theta) = 2V(R, \Theta)$ [12,43]. Because of the variation in $\gamma(R, \Theta)$, the predicted evolution for the ensemble exhibits a monotonic increase and saturation, but no observable Rabi oscillations. Measurements of the remaining pp population in an experimental ensemble show a corresponding monotonic decrease (black dots in Figs. 2 and 3).

The situation is similar when the atom pairs are detuned from resonance by an energy E. The oscillations in the transition probability for individual atom pairs, at generalized Rabi frequencies $\Gamma(R, \Theta) = \sqrt{E^2 + 4V^2}$ [43], are again obscured in the ensemble average, leading to an initial increase (decrease) and then saturation of the ss' (pp) population (magenta dots in Figs. 2 and 3). The primary differences from the on-resonant case being a
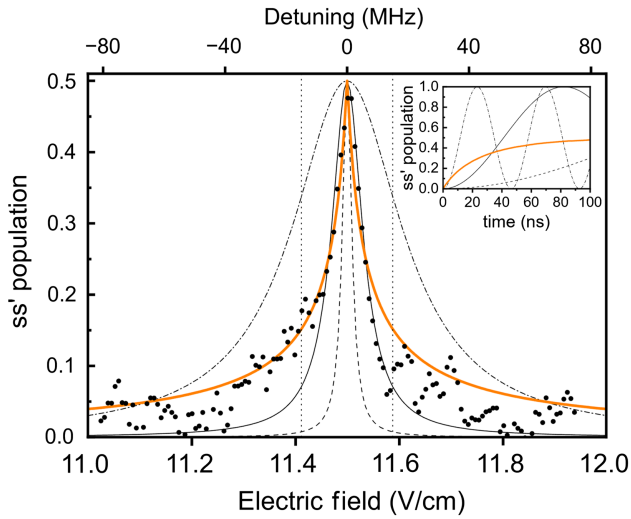

FIG. 1. Dipole-dipole driven population transfer probability vs applied electric field (lower axis) and bare-state energy splitting (upper axis). Black dots: experimental result for a 500 ns interaction time and $\rho = 2 \times 10^9$ cm^{-3}. Solid orange: simulated cusp line shape for the ensemble [19], including nearest-neighbor Rydberg interactions only [24]. Thin black lines: predicted Lorentzian line shapes for atom pairs with DD couplings corresponding to 20% (dashed), 50% (solid), and 80% (dot-dashed) levels in the ensemble integrated coupling-strength probability distribution. The vertical dotted lines mark the ± detuning points for a typical control sequence. Inset: simulated population transfer vs interaction time with the system tuned to resonance for 500 ns, and line types corresponding to those in the main figure.
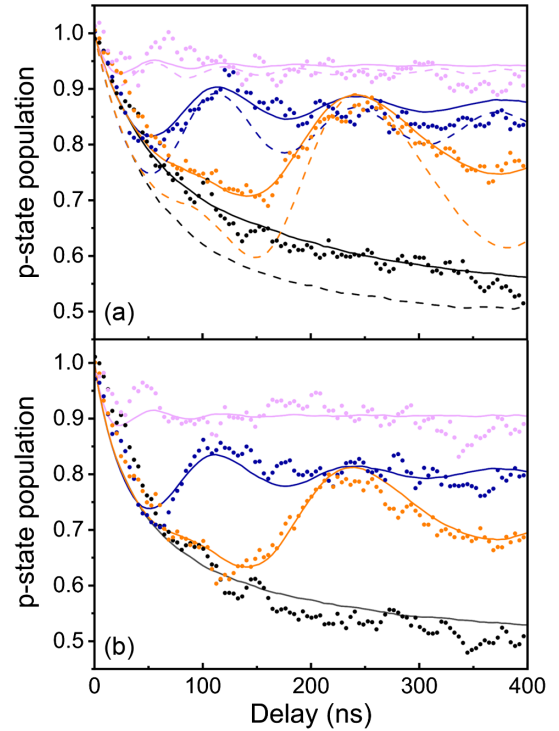

FIG. 2. Experimental results (dots), along with 2-atom [dashed lines, Fig. 2(a) only] and 4-atom (solid lines) simulations, for p state population (normalized to total population) as a function of delay T after an ensemble of initially excited p atoms with peak Rydberg density (a) 1×10^9/cm^3 and (b) 2×10^9/cm^3 is tuned on-resonance (black) or +15 MHz (magenta) on the positive field side of resonance for $t > 0$, or subjected to QPM sequences with a total of $N = 2$ (blue) or $N = 4$ (orange) time zones with alternating detunings of ±15 MHz. In (a) and (b), $E/E_0 \simeq 5$ and 2.5, respectively. There are no adjustable parameters in the simulations. All data in each graph have been scaled using a single normalization constant.
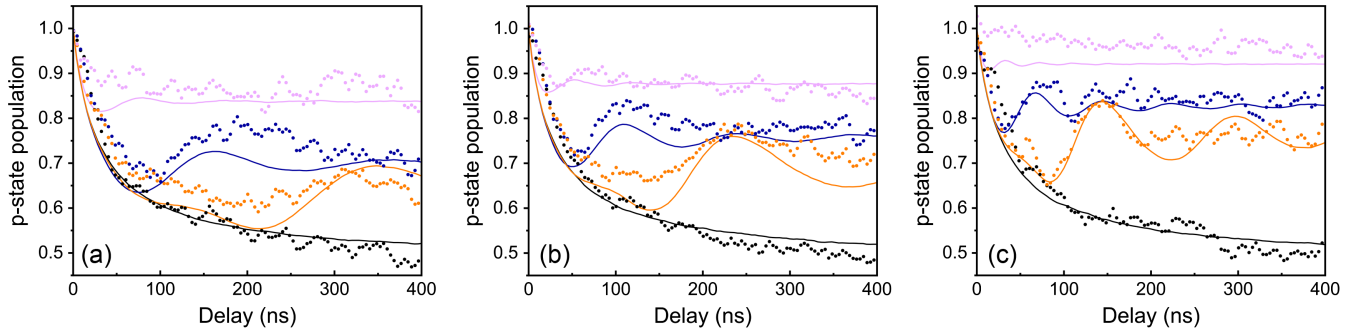
FIG. 3.   Analogous to Fig. 2 except that the Rydberg density is fixed at $3 \times 10^9/\text{cm}^3$ ($E_0 \simeq 9$ MHz) with detuning magnitudes of (a) $E = 10$ MHz, (b) $E = 15$ MHz, and (c) $E = 25$ MHz.

decrease in the maximum ensemble-averaged transition probability, $\langle 4V^2/\Gamma^2 \rangle$, and a more rapid saturation due to the increase in Γ.

In the remainder of this Letter we use the visibility of Rabi oscillations as a metric for the effectiveness of control sequences for suppressing the impact of inhomogeneities in the coupling strength on coherent state preparation across the ensemble. Our principal goal is to reduce the variation $\Delta\phi$ in the Rabi phase, $\phi = \Gamma T$, acquired by different atom pairs interacting for the same time T, enabling the creation of (more) uniform distributions of arbitrary quantum superpositions of pp and ss' pair states.

Since the variation ΔV in the interaction strength within the random ensemble is comparable to V_0, the half-width E_0 of the ensemble-averaged population transfer cusp line shape provides a reasonable measure of ΔV. On resonance, the phase variation $\Delta\phi = E_0 T$ is a maximum, resulting in the greatest dephasing for a given interaction time T. However, if all atom pairs have the same large detuning $|E| \gg E_0$, then $\Delta\phi \approx T E_0^2/(2E)$, and there is negligible dephasing for times $T \ll 2E/E_0^2$. Of course, with large detunings, the maximum ensemble-averaged transition probability, $\langle 4V_0^2/\Gamma^2 \rangle \sim E_0^2/E^2$, is also negligibly small. Therefore, interactions at large detuning alone are not an option for creating ensembles of atoms in identical arbitrary quantum superposition states.

Off resonance, the transition amplitude is limited by the relative phase mismatch between the coupled states, which advances at a rate E. A similar effect caps optical harmonic conversion in nonlinear crystals where harmonic and fundamental waves travel with different indices of refraction. In that case, quasi-phase-matching (QPM) via periodic poling [20], characterized by a reversal of the sign of the nonlinear susceptibility at regular intervals within the crystal, can dramatically increase the conversion efficiency. We demonstrate an analogous approach, periodically flipping the sign of E to implement a time-domain variant of QPM in a driven quantum system. *This enables large transition amplitudes at any detuning.*

Figures 2 and 3 show the evolution of the pp character when QPM sequences are applied to a DD-driven

many-atom Rydberg gas. During the sequence, the initial $32p$ ensemble is subjected to periodic electric field steps or "jumps" that rapidly (~ 2 ns) tune the atom pairs back and forth across the resonance, reversing the sign of E. The atoms interact with alternating detunings $\pm E$ in N adjacent time "zones," each with a duration T/N, for a total time T [44].

Several features of the data in Figs. 2 and 3 illustrate the effectiveness of the control sequences for reducing dephasing within the ensemble while allowing for large probability amplitude transfers. First, the level of off-resonant coherent population transfer is substantially enhanced through QPM, increasing with N so that large detunings can be used to reduce dephasing without limiting the range of constituent state amplitudes that can be realized. Second, Rabi oscillations that are completely obscured in the on-resonant (black) and constant detuning (magenta) data are revealed through QPM. To our knowledge this is the first observation of DD-driven Rabi oscillations in a random ensemble with more than a few atoms. As expected for large detunings, the period of the damped Rabi oscillations is largely independent of density (Fig. 2) and inversely proportional to $\Gamma \simeq E$ (Fig. 3). Interestingly, the oscillation period and damping time increase in proportion to the number of QPM zones.

The principal characteristics of the data in Figs. 2 and 3 are captured by numerical simulations [24,45]. The calculations follow the quantum evolution of 5000 individual groups of two (dashed lines) or four (solid lines) nearest-neighbor $32p$ atoms that are selected from within a random ensemble at the measured densities. The atoms in each group are allowed to interact for a total time T and the probabilities for finding atoms in the initial $32p$ state are summed over the individual groups. All atom pairs are subject to the (near) resonant $pp \leftrightarrow ss'$ Förster interaction for the constant or periodically reversing detuning. Pairs of atoms within the four atom groups are also subject to field-independent DD-exchange interactions, $ps \leftrightarrow sp$ and $ps' \leftrightarrow s'p$ [24], which are partially suppressed by the resonant interactions between nearest neighbors [15,17,45]. While ignoring exchange provides qualitative agreement

with the data [dashed lines in Fig. 2(a)], a quantitative comparison requires its inclusion in the four atom model [24,45].

The good quantitative agreement between experiment and theory in Fig. 2 suggests that the few atom model captures the essential physics underlying the evolution of the DD-coupled Rydberg gas with, and without, the control sequences, particularly at lower Rydberg densities. At the higher density used in Fig. 3, the accuracy of the four atom model is reduced and the agreement with experiment is less impressive. Specifically, the increase in atom-atom coupling strength decreases the relevant interaction timescales so that the 2 ns duration of the field step is not totally negligible. In addition, excitation hopping outside of four atom groups is more probable at earlier times within the 400 ns observation window. Still, the agreement is sufficient to support our interpretation of the control dynamics. Indeed, more insight into how QPM actively suppresses dephasing, the explicit form of the observed N dependence of the amplitude and frequency of the Rabi oscillations, and even our rationale for describing the observed modulations as Rabi oscillations (rather than a more generic interference effect) is better obtained from approximate analytic expressions describing the two-level quantum state evolution within isolated nearest-neighbor atom pairs.

Applying the standard state transformation for a coherently coupled two-level system, the population transfer probability from pp to ss' exhibits Rabi oscillations, $P_{ss'}(T) = (2V/\Gamma)^2 \sin^2(\frac{1}{2}\Gamma T)$ as a function of the interaction time T [24,46]. Successive application of that state transformation, describing a QPM sequence in which the sign of the detuning alternates in N successive time zones of duration T/N [assuming $E \gg V$ and $P_{ss'}(T) \ll 1$], obtains an identical expression for $P_{ss'}(T)$, provided Γ is replaced with Γ/N [24]. Thus, we refer to the observed modulations as Rabi oscillations. The predicted proportionality between the Rabi period and N is a clear feature of the data and simulations in Figs. 2 and 3. The observed enhancement in $P_{ss'}(T)$ is not as large as the predicted factor of N^2, due to a breakdown of the assumption $P_{ss'}(T) \ll 1$ (also responsible for the deviation from purely sinusoidal modulations) and to non-negligible contributions from atom pairs with smaller than average separations (and $E \sim V$) [47].

Two principal factors are responsible for the suppression of dephasing through QPM. First, as discussed previously, the variation in Γ is significantly smaller for $|E| \gg E_0$, resulting in a substantial reduction in the ensemble phase variation $\Delta\phi$ over any time interval. Second, since the phase evolution is reversed in successive time zones (similar to a spin echo [48]), $\Delta\phi$ does not accrue over the total interaction time T. The effect is distinct from an echo, however, because the coupling is present throughout the system evolution and the relative phase φ between the superimposed pp and ss' states advances at a nonconstant

rate within each zone. At the end of each zone in a QPM sequence, the magnitude of $\Delta\phi$ is equal to that at the completion of zone 1, acquired during the interval T/N [24]. Accordingly, if the ensemble dephases after a time $T = \tau$ while at constant detuning, then, with a QPM sequence, it will not dephase until the time spent in zone 1 is $T/N = \tau$, i.e., until the total interaction time is $T = N\tau$. Thus, QPM extends the dephasing time by a factor of N.

Figures 2 and 3 clearly show the predicted extension of the dephasing time with increasing N. Interestingly, since the dephasing time and Rabi frequency are proportional to N and $1/N$, respectively, their product, which gives the number of Rabi cycles that can be observed within the dephasing time, is independent of N. The data and simulation show that this relationship continues to hold for $E \sim E_0$ and $P_{ss'}(T) \sim 1$.

QPM sequences can be even more effective at suppressing dephasing in systems with narrower coupling-strength distributions. One example is an ensemble of resonantly driven atoms near the center of a Gaussian laser beam [7–9]. Another involves interactions between trapped atoms (or ions) whose separations are relatively well-defined. Simulations analogous to those we have used for random ensembles illustrate the effectiveness of QPM sequences for creating a uniform ensemble of quantum states in DD-coupled atom pairs (e.g., held in optical tweezer arrays) with a narrow spread in R [24].

In the future, QPM may also be employed to suppress microscopic decoherence resulting from time-dependent changes in V for individual elements in an ensemble. These may be caused, for example, by relative thermal motion of atoms or the spatial jitter of a laser beam or trap array. Given the reversal of the phase advance in successive QPM zones, decoherence caused by temporal variations in V (integrated over a total interaction time T) can be minimized through the use of a sufficient number of QPM zones with negligible changes in V during the time T/N spent in each zone [25].

[1] T. M. Weber, M. Höning, T. Niederprüm, T. Manthey, O. Thomas, V. Guarrera, M. Fleischhauer, G. Barontini, and H. Ott, Nat. Phys. **11**, 157 (2015).

[2] Y. Mei, Y. Li, H. Nguyen, P. R. Berman, and A. Kuzmich, Phys. Rev. Lett. **128**, 123601 (2022).

[3] Y. Li, Y. Mei, H. Nguyen, P. R. Berman, and A. Kuzmich, Phys. Rev. A **106**, L051701 (2022).

[4] J. A. Hines, S. V. Rajagopal, G. L. Moreau, M. D. Wahrman, N. A. Lewis, and O. Marković, and M. Schleier-Smith, Phys. Rev. Lett. **131**, 063401 (2023).

[5] L. Ji, Y. He, Q. Cai, Z. Fang, Y. Wang, L. Qiu, L. Zhou, S. Wu, S. Grava, and D. E. Chang, Phys. Rev. Lett. **131**, 253602 (2023).

[6] I. Tsiamis, O. Kyriienko, and A. S. Sørensen, arXiv:2309.10873.

[7] M. Reetz-Lamour, J. Deiglmayr, T. Amthor, and M. Weidemüller, New J. Phys. **10**, 045026 (2008).

[8] J. Deiglmayr, M. Reetz-Lamour, T. Amthor, S. Westermann, A. de Oliveira, and M. Weidemüller, Opt. Commun. **264**, 293 (2006).

[9] T. Cubel, B. K. Teo, V. S. Malinovsky, J. R. Guest, A. Reinhard, B. Knuffman, P. R. Berman, and G. Raithel, Phys. Rev. A **72**, 023405 (2005).

[10] T. Förster, Z. Naturforsch. A **4**, 321–327 (1949).

[11] T. G. Walker and M. Saffman, J. Phys. B **38**, S309 (2005).

[12] S. Ravets, H. Labuhn, D. Barredo, L. Béguin, T. Lahaye, and A. Browaeys, Nat. Phys. **10**, 914 (2014).

[13] W. R. Anderson, J. R. Veale, and T. F. Gallagher, Phys. Rev. Lett. **80**, 249 (1998).

[14] I. Mourachko, D. Comparat, F. de Tomasi, A. Fioretti, P. Nosbaum, V. M. Akulin, and P. Pillet, Phys. Rev. Lett. **80**, 253 (1998).

[15] B. Sun and F. Robicheaux, Phys. Rev. A **78**, 040701(R) (2008).

[16] S. Westermann, T. Amthor, A. L. de Oliveira, J. Deiglmayr, M. Reetz-Lamour, and M. Weidemüller, Eur. Phys. J. D **40**, 37 (2006).

[17] K. C. Younge, A. Reinhard, T. Pohl, P. R. Berman, and G. Raithel, Phys. Rev. A **79**, 043420 (2009).

[18] I. I. Ryabtsev, D. B. Tretyakov, I. I. Beterov, and V. M. Entin, Phys. Rev. Lett. **104**, 073003 (2010).

[19] B. G. Richards and R. R. Jones, Phys. Rev. A **93**, 042505 (2016).

[20] I. A. Armstrong, N. Bloembergen, I. Ducuing, and P. S. Pershan, Phys. Rev. **127**, 1918 (1962).

[21] E. Guardado-Sanchez, P. T. Brown, D. Mitra, T. Devakul, D. A. Huse, P. Schauß, and W. S. Bakr, Phys. Rev. X **8**, 021069 (2018).

[22] H. Labuhn, D. Barredo, S. Ravets, S. de Léséleuc, T. Macrì, T. Lahaye, and A. Browaeys, Nature (London) **534**, 667 (2016).

[23] H. Bernien, S. Schwartz, A. Keesling, H. Levine, A. Omran, H. Pichler, S. Choi, A. S. Zibrov, M. Endres, M. Greiner, V. Vuletić, and M. D. Lukin, Nature (London) **551**, 579 (2017).

[24] See Supplemental Material at http://link.aps.org/supplemental/10.1103/PhysRevLett.132.043201 for more information, which includes Refs. [25–39].

[25] M. R. Kutteruf and R. R. Jones, Phys. Rev. Lett. **108**, 013001 (2012).

[26] P. Hertz, Math. Ann. **67**, 387 (1909).

[27] S. Chandrasekhar, Rev. Mod. Phys. **15**, 1 (1943).

[28] F. Robicheaux, J. V. Hernandez, T. Topcu, and L. D. Noordam, Phys. Rev. A **70**, 042703 (2004).

[29] G. Racah, Phys. Rev. **62**, 438 (1942).

[30] A. R. Edmonds, *Angular Momentum in Quantum Mechanics*, Princeton Landmarks in Mathematics and Physics (Princeton University Press, Princeton, NJ, 1996).

[31] E. A. Yakshina, D. B. Tretyakov, I. I. Beterov, V. M. Entin, C. Andreeva, A. Cinins, A. Markovski, Z. Iftikhar, A. Ekers, and I. I. Ryabtsev, Phys. Rev. A **94**, 043417 (2016).

[32] W. Li, I. Mourachko, M. W. Noel, and T. F. Gallagher, Phys. Rev. A **67**, 052502 (2003).

[33] L. Viola and S. Lloyd, Phys. Rev. A **58**, 2733 (1998).

[34] L. Viola, E. Knill, and S. Lloyd, Phys. Rev. Lett. **82**, 2417 (1999).

[35] D. Vitali and P. Tombesi, Phys. Rev. A **59**, 4178 (1999).

[36] C. Search and P. R. Berman, Phys. Rev. Lett. **85**, 2272 (2000).

[37] R. S. Minns, M. R. Kutteruf, H. Zaidi, L. Ko, and R. R. Jones, Phys. Rev. Lett. **97**, 040504 (2006).

[38] R. S. Minns, M. R. Kutteruf, M. A. Commisso, and R. R. Jones, J. Phys. B **41**, 074012 (2008).

[39] E. Bauch, C. A. Hart, J. M. Schloss, M. J. Turner, J. F. Barry, P. Kehayias, S. Singh, and R. L. Walsworth, Phys. Rev. X **8**, 031025 (2018).

[40] T. J. Carroll, K. Claringbould, A. Goodsell, M. J. Lim, and M. W. Noel, Phys. Rev. Lett. **93**, 153001 (2004).

[41] T. F. Gallagher, *Rydberg Atoms* (Cambridge University Press, Cambridge, England, 1994).

[42] M. D. Lukin, M. Fleischhauer, R. Cote, L. M. Duan, D. Jaksch, J. I. Cirac, and P. Zoller, Phys. Rev. Lett. **87**, 037901 (2001).

[43] Analytic expressions for the coherent evolution of DD-coupled atom pairs in terms of the amplitudes in the pp and ss' basis states are straightforward to derive [24].

[44] Population transfer resulting from asymmetric jump sequences in which negligible time is spent at either $\pm$ detuning is indistinguishable from that obtained at constant detuning. The distinctive characteristics of the QPM data are due to the coherent DD interactions within each zone, not on the transitions between zones.

[45] C. He, Quantum control of cold Rydberg ensembles and non-Hermitian systems, Ph.D. thesis, University of Virginia, Charlottesville, VA, 2021.

[46] P. Meystre and M. Sargent III, *Elements of Quantum Optics*, 4th ed. (Springer, New York, 2007).

[47] Visualization of the Bloch sphere evolution of the state vectors for individual atom pairs provides additional insight into the origin of the $1/N$ Rabi frequency scaling and the mechanism underlying active dephasing suppression with QPM [24].

[48] E. L. Hahn, Phys. Rev. **80**, 580 (1950).